Respiratory Physiology & Neurobiology 270 (2019) 103282

Contents lists available at ScienceDirect

Respiratory Physiology & Neurobiology

journal homepage: www.elsevier.com/locate/resphysiol

# sFRP2 promotes airway inflammation and Th17/Treg imbalance in COPD via Wnt/β-catenin pathway

Miao Zhou[a,*,1], Li Jiao[a,1], Yuanyuan Liu[b]

[a] Department of lung disease division, Third Affiliated Hospital of Henan University of Traditional Chinese Medicine, Zhengzhou, 450008, China
[b] College of Acupuncture-moxibustion and Tuina, Henan University of Chinese Medicine, Zhengzhou, 450008, China

ARTICLE INFO

*Keywords:*
Chronic obstructive pulmonary disease
sFRP2
Airway inflammation
Th17/Treg balance1

ABSTRACT

Imbalance between inflammatory Th17 cells and immunosuppressive regulatory T cells (Treg) contributes to the progression of chronic obstructive pulmonary disease (COPD). We aims to investigate roles and mechanisms of secreted frizzled-related protein 2 (sFRP2) in airway inflammation and Th17/Treg differentiation in COPD. sFRP2 was significantly upregulated in the serum of patients with COPD and in human bronchial epithelial (HBE) cells that were exposed to cigarette smoke extract (CSE). sFRP2 was negatively correlated with FEV1/FVC. CSE increased IL-6 and TNF-α in HBE cells, which was reversed by sFRP2 silencing. CSE exposure elevated the percentage of Th17 in $CD3^+$ $CD8^-$ cells while reduced the percentage of Treg in $CD4^+CD25^+$ cells. Knockdown of sFRP2 in peripheral blood mononuclear cells (PBMCs) attenuated Th17 differentiation and induced Treg differentiation. CSE suppressed the expression of β-catenin and Cyclin D1 in PBMCs while knockdown of sFRP2 markedly reversed the inhibitory effects of CSE. Wnt/β-catenin inhibition by Dickkopf-1 reversed the inhibitory effect of si-sFRP2 on the production of inflammatory cytokines and imbalance between Th17 and Treg cells caused by CSE. CSE induced sFRP2 potentiated airway inflammation and disturbed Th17/Treg homeostasis by inhibiting β-catenin.

## 1. Introduction

Chronic obstructive pulmonary disease (COPD) is a progressive lung disease characterized by incompletely reversible airflow limitation and usually caused by exposure to harmful gases or particles (Vogelmeier et al., 2017). COPD is the third-leading cause of mortality worldwide (Capozzolo et al., 2017). Prevalence of COPD in adults increases with age and more than 27% of the patients are over 60 years old, making it a major disease burden in China (Wang et al., 2018). The pathogenesis of COPD includes oxidative stress, protease and anti-protease imbalance, inflammation and fibrosis. Inflammatory, epithelial, and other structural cells jointly release inflammatory mediators during COPD pathogenesis (Barnes, 2016).

Adaptive immune responses, specifically those mediated by T cells, may contribute to COPD (Saetta et al., 1993). In addition to T helper (Th) cells Th1 and Th2, extensive studies show that Th17 and regulatory T cell (Treg) subsets also help to maintain immune homeostasis in COPD (Wang et al., 2015; Weaver and Hatton, 2009). Wang et al. reported higher frequency of Th17 and lower frequency of Tregs in patients with COPD, compared with that in healthy non-smokers or healthy smokers(Wang et al., 2015). Increased Th17 is inversely correlated with forced expiratory volume in one second (FEV1) and forced vital capacity (FVC) and is linked to severity of airflow limitation (Vargas-Rojas et al., 2011). Increased Th17 cell levels are inversely correlated with low Treg level in COPD, suggesting that imbalance between Th17 cells and Tregs is associated with COPD progression (Li et al., 2014). However, the factors mediate the disturbance of Th17/Treg remain unclear.

Secreted frizzled-related proteins (sFRPs) form a family of secreted glycoproteins containing a cysteine-rich domain that is highly homologous to Wingless-type (Wnt) ligands. Therefore, sFRPs inhibit the Wnt/β-catenin pathway by competitively binding Wnt ligands of the frizzled protein receptor. Secreted frizzled-related protein 2 (sFRP2) belongs to this glycoprotein family. It is implicated in diverse extracellular regulatory processes, including tumorigenesis and embryogenesis. It also reportedly modulates epithelial-mesenchymal transition and stemness (Zeng et al., 2018).

Frequent methylation and silencing of sFRP1, sFRP2, and sFRP5 occurs in hepatocellular carcinoma, suggesting that their loss of function contribute to hepatocarcinogenesis (Takagi et al., 2008).

* Corresponding author.
*E-mail address:* miaozhouldd@163.com (M. Zhou).
[1] These authors contributed equally to this work.

https://doi.org/10.1016/j.resp.2019.103282
Received 19 March 2019; Received in revised form 16 August 2019; Accepted 16 August 2019
Available online 17 August 2019
1569-9048/ 

Importantly, in a rat model of rheumatoid arthritis, sFRP2 was significantly downregulated, resulting in expression of IL-6 and IL-8. DNA methylation of sFRP2 affected the pathogenesis of rheumatoid arthritis via canonical Wnt signaling, indicating the important role of sFRP2 in autoimmune disease (Miao et al., 2018). However, the molecular mechanisms of sFRP2 in COPD remain unexplored.

In the current study, we examined the role of sFRP2 in airway inflammation and COPD development in epithelial cells stimulated by cigarette smoke extract (CSE). We also assessed the expression of sFRP2 in peripheral blood samples from patients with COPD and knockdown of sFRP2 on the differentiation of Th17 and Treg cells in peripheral blood mononuclear cells (PBMCs) exposed to CSE.

## 2. Materials and methods

### 2.1. Subjects

We enrolled 17 healthy nonsmokers, 17 healthy smokers, and 17 patients with COPD. The COPD was diagnosed based on the Global Initiative for Chronic Obstructive Lung Disease (GOLD) criteria (Vestbo et al., 2013). Participants had no significant difference in age, gender, or body mass index among the three groups. The ethics committee of Third Affiliated Hospital of Henan University of Traditional Chinese Medicine approved this study.

### 2.2. Cigarette smoke extract preparation

CSE was prepared according to a previously described method with minor modification (Ballweg et al., 2014). Briefly, research-grade cigarettes were bubbled through 100 ml of RPMI 1640 medium at constant airflow. Subsequently, the pH value of the medium was adjusted to 7.4, and the medium was sterile-filtered through a 0.22-μm filter to remove bacteria and large particles. The resulting solution served as 100% CSE and was further diluted to indicated concentrations.

### 2.3. Cell culture and treatment

Human lung bronchial epithelial (HBE) line were obtained from ATCC (Carlsbad, CA, USA). Cells were cultured in RPMI 1640 supplemented with 10% fetal bovine serum. Finally, cells were treated for 48 h with 1%, 2.5%, 5%, or 10% CSE or with 10% CSE for 24 h, 48 h, or 72 h to detect the treatment dose and time effects of CSE on sFRP2 expression.

### 2.4. MTT assay

Conventional MTT assay was used to determine the cell viability in response to the stimulation by different dose of CSE. Cells were cultured in 96-well plates at a density of $2.0 \times 10^5$ cells per well and treated with CSE (1%, 2.5%, 5%, or 10%) for 48 h. Then 20 μL of MTT stock solution (5 mg/mL) was added, and cells were incubated at 37 °C for another 4 h. The resulting MTT formazan was extracted with 150 μL of dimethyl sulfoxide. Absorbance was detected using a microtiter plate reader at 490 nm. The cell viability was calculated as a percentage to the absorbance in control (set as 100%).

### 2.5. Cell transfection

HBE cells and PBMCs were transfected with sFRP2 small interfering RNA (si-sFRP2) at concentrations of 40, 60 and 80 nM or a negative control siRNA (si-NC) using Lipofectamine 2000 (Invitrogen, Carlsbad, CA, USA), according to the manufacturer's protocol. Transfection efficiency was determined by western blot assay at 48 h after transfection.

### 2.6. Measurement of sFRP2 and cytokines in the supernatant

After reaching confluence to 90%, HBE cells were treated with the indicated dose at the indicated time. TNF-α and IL-6 in the supernatant of the cell culture were measured using the appropriate commercially available ELISA kits (R&D Systems, Los Angeles, CA, USA). Human serum sFRP2 level was measured using a sFRP2 ELISA kit (USCN, Wuhan, China). Absorbance at 450 nm was examined using a microplate reader.

### 2.7. Quantitative RT-PCR

Total RNA was isolated from HBEs using Trizol reagent according to the manufacturer's instructions. Then 0.5 μg of RNA was used to generate cDNA using a PrimeScript RT reagent kit (Takara, Dalian, China). Afterward, quantitative real-time PCR was performed using SYBR Premix Ex Taq (Takara). Each 20-μl well reaction comprised 10 μl of SYBR Green (Invitrogen), 0.4 μl of forward primer, 0.4 μl of reverse primer, 2 μl of cDNA, and corresponding $ddH_2O$. Relative gene expression was calculated using the $2^{-\Delta\Delta Ct}$ method. β-actin was used as the housekeeping gene. The forward primer of human sFRP2 was 5′-CTGCCACCGCTTCACCGAGG-3′ and the reverse primer of sFRP2 was 3′−CCAGCCACCGAGGAAGCTCCA-5′. Besides, the resulted PCR products was electrophoresed on 1% agarose gel and visualized by the Gel Imaging System of Bio-Rad Corp (Bio-Rad, Hercules, CA, USA).

### 2.8. Western blot analysis

Cells were lysed with RIPA buffer, and the protein concentration was determined using a BCA protein assay kit (Thermo Fisher Scientific, Waltham, MA, USA). Then, equal amounts of protein were subjected to 10% SDS–polyacrylamide gel electrophoresis and transferred onto PVDF membranes. Afterwards, the membranes were blocked with 5% non-fat milk in PBS containing 0.01% Tween for 1 h at room temperature and followed by incubation overnight with appropriate primary antibodies at 4 °C. Membranes then were incubated with HRP-conjugated secondary antibodies for 1 h at room temperature. Bands of interest were visualized using an enhanced chemiluminescence system and analyzed with Image *J*software. The following antibodies were used in this study: anti-sFRP2 (Santa Cruz Biotechnology, CA, USA), anti-cyclin D1 (Santa Cruz Biotechnology), anti-β-catenin (Santa Cruz Biotechnology), and anti-β-actin (Sigma, St. Louis, MO, USA).

### 2.9. Immunofluorescence staining

PBMCs were seeded and incubated overnight onto glass cover slips at a density of 1˜4 × $10^4$ cells/well. After treatment, cells were fixed in 95% methanol solution. Primary antibodies against β-catenin (1:250) and cyclin D1 (1:200) (Abcam, Cambridge, UK) were diluted in blocking buffer and incubated at 4 °C overnight. The resulted cells were washed in PBS and incubated with secondary antibodies as appropriate (1:2000, Invitrogen) for 1 h at room temperature. Cells were then washed in PBS and mounted in Prolong Gold anti-fade reagent containing DAPI (Invitrogen). Images were captured on a Leica TCS SP5 II scanning laser confocal system.

### 2.10. Flow cytometry

PBMCs were isolated from individual participants via Ficoll density gradient centrifugation. To determine the frequency of $CD4^+$ $CD25^+$ $Foxp3^+$ Tregs, PBMCs ($2 \times 10^6$ cells/mL) were stained with fluorescein isothiocyanate (FITC)-labeled anti-human CD4 and APC-labeled anti-human CD25 antibodies for 30 min, followed by fixing, permeabilization, and staining with PE-labeled anti-human Foxp3 or isotype control (eBioscience, San Diego, CA, USA). To determine the frequency of $CD3^+$ $CD8^-$ $IL^-17^+$ Th17 cells, PBMCs ($2 \times 10^6$ cells /mL) were

stimulated at room temperature for 4 h with 50 ng/mL of phorbol 12-myristate 13-acetate (PMA, Sigma-Aldrich, St. Louis, USA) and 500 ng/mL of ionomycin (Sigma-Aldrich) in the presence of brefeldin A (2.5 μg/mL; Sigma-Aldrich) and 10% fetal calf serum. Then, cells were harvested and stained with FITC-labeled anti-human CD3 and APC-labeled anti-human CD8 at 4 °C for 30 min, followed by fixing, permeabilization, and then staining with PE-labeled anti-human IL-17A (eBioscience). FACS Canto II (BD Biosciences, Franklin Lakes, NJ, USA) was used for cell analysis. Data analysis was performed using CellQuest software (BD Corporation).

### 2.11. Statistical analysis

Statistical analyses were performed using SPSS 22.0. All data are presented as mean ± SD. A *t* test was used for comparison between the two groups and one-way analysis of variance (ANOVA) followed by Bonferroni post hoc tests for multiple comparisons. $P < 0.05$ were considered statistically significant.

## 3. Results

### 3.1. Increased serum sFRP2 in patients with chronic obstructive pulmonary disease

To investigate the role of sFRP2 in COPD, we detected sFRP2 in the serum of patients with COPD. As shown in Fig. 1A, compared with the healthy nonsmoker (HC) group and healthy smoker (HS) groups, sFRP2 increased 5-fold and 3-fold in the sera of the COPD group, respectively. Additionally, sFRP2 was negatively correlated with FEV1/FVC (r = -0.570, $P = 0.017$; Fig. 1B). These results suggest a potential role of sFRP2 in COPD.

### 3.2. Cigarette smoke extract upregulated expression of sFRP2 in human lung bronchial epithelial cells

To further explore expression of sFRP2 in COPD, we treated HBE cells with 1%, 2.5%, 5%, or 10% CSE for 48 h. It was shown that cell viability gradually decreased against the increase of CSE concentrations, and exposure of 2.5% CSE or above significantly suppressed cell viability (Fig. 1C). RT-PCR and western blot analysis showed that CSE induced expression of sFRP2 in a concentration-dependent manner (Fig. 1D–F). Further analysis demonstrated that sFRP2 increased in a time-dependent manner from between 24 h to 72 h (Fig. 1G–I).

### 3.3. sFRP2 altered levels of cellular inflammatory factors

In order to detect the effect of sFRP2 on CSE-evoked inflammation in HBE cells, we transfected different dose of si-sFRP2 to HBE cells before CSE stimulation and confirmed their transfection efficiency using RT-PCR and western blotting. It was demonstrated that the mRNA and protein levels of sFRP2 prominently decreased after 40 nM to 80 nM sFRP2-siRNA transfection, and 60 nM si-sFRP2 achieved the optimal inhibitory effect on sFRP2 (Fig. 2A and B). Additionally, an ELISA assay revealed higher levels of inflammatory cytokines IL-6 and TNF-a in the supernatant of CSE group, compared to those in the control group ($P < .05$, Fig. 2D and E). However, knockdown of sFRP2 reversed the increased expression of IL-6 and TNF-a induced by CSE (Fig. 2C and D). These results indicated that sFRP2 inhibition reduced inflammation.

### 3.4. sFRP2 promoted Th17 cell and suppressed Tregs in vitro

To investigate the effect of sFRP2 on Treg cells and Th17 cells differentiation, PBMCs were transfected with 60 nM si-sFRP2 and then

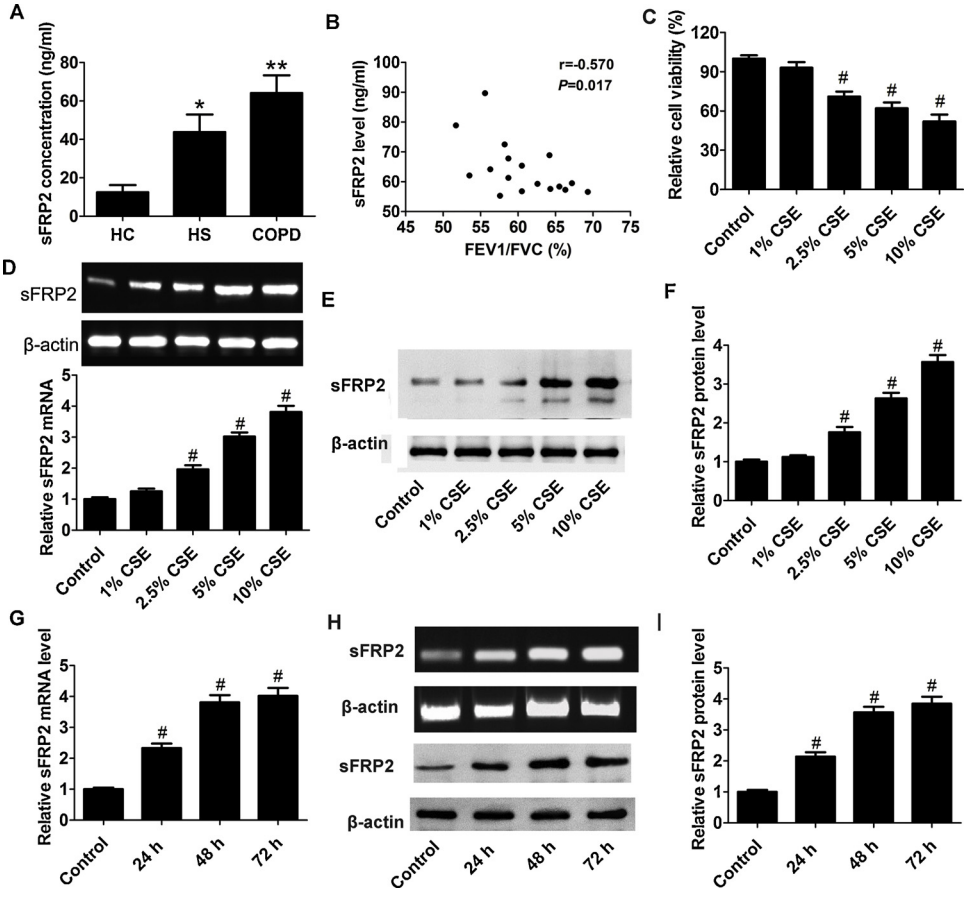


**Fig. 1.** sFRP2 increased in the sera of patients with chronic obstructive pulmonary disease and in human lung bronchial epithelial cells exposed to cigarette smoke extract. (A) Expression of sFRP2 in the sera of healty nonsmokers (HC), healthy smokers (HS), and patients with chronic obstructive pulmonary disease were analyzed using an ELISA kit. (B) Correlation between sFRP2 expression and lung function parameter FEV1/FVC%. HBE cells were exposed to cigarette smoke extract (CSE) at the concentration of 0%, 1%, 2.5%, 5%, and 10% for 48 h. (C) Relative HBE cell viabilities to non-treated control were determined using MTT assays; (DF−) The mRNA and protein levels of sFRP2 were determined by RT-qPCR and Western blot, respectively. HBE cells were exposed to cigarette smoke extract (CSE) at the concentration of 10% for 24 h, 48 h and 72 h. (GI−) The mRNA and protein levels of sFRP2 were determined by RT-qPCR and western blot, respectively, and the representative images of sFRP2 levels detected by agarose gel electrophoresis and western blot were shown. $^{*}P < .05$ and $^{**}P < .01$ versus the HC group; $^{\#}P < .05$ versus the control group.

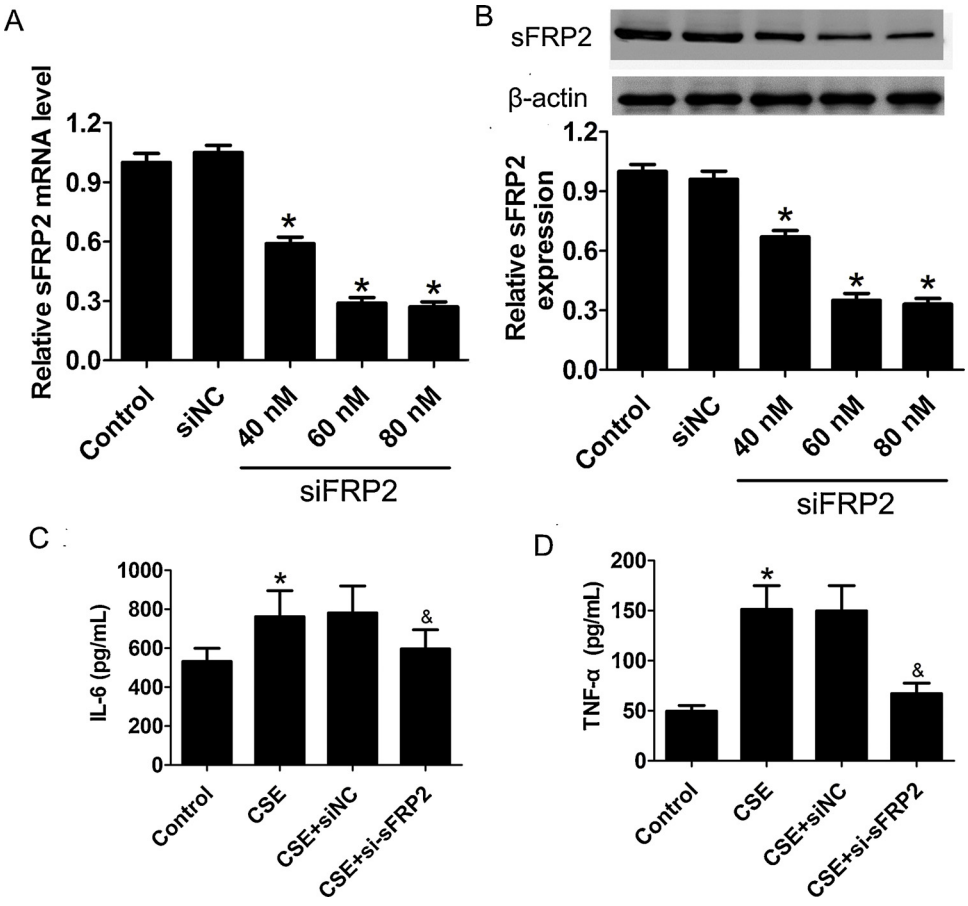


**Fig. 2.** Knockdown of sFRP2 suppressed inflammation caused by cigarette smoke extract in human lung bronchial epithelial cells. Human lung bronchial epithelial cells were transfected with sFRP2 siRNA (si-SFRP2) at final concentrations of 40, 60 and 80 nM in 1 mL medium for 48 h and then exposed to 10% cigarette smoke extract for 48 h. (AB—) The mRNA and protein levels of sFRP2 were analyzed using RT-qPCR and western blot, respectively. Inflammatory cytokines (C and D) IL-6 and TNF-α in the supernatant of the cell culture were analyzed using corresponding ELISA kits. $^{*}P < .05$ versus the control group; $^{\&}P < .05$ versus the CSE + si-NC group. Data represent results from four independent experiments.

exposed to 10% CSE for 24 h. Flow cytometry showed that CSE significantly increased the ratio of Th17 in $CD3^{+}CD8^{-}$ cells (Fig. 3A and B). Alternatively, CSE reduced the frequency of Treg cells in $CD4^{+}CD25^{+}$ cells (Fig. 3A and C), whereas CSE exposure resulted in a significant increase in the ratio of Th17 and Treg cells (Fig. 3D). However, knockdown of sFRP2 significantly reversed the effect of CSE on Th17, Treg, and the Th17/Treg proportion, as indicated by the decreased frequency of Th17 cells, the increased frequency of Treg cells, and the decreased ratio of Th17/Treg cells (Fig. 3A–D). These results demonstrate that sFRP2 in $CD4^{+}$ T cells promoted Th17 cell differentiation and inhibited generation of Treg cells.

### *3.5. sFRP2 decreased the Wnt/β-catenin signaling in PBMCs stimulated by cigarette smoke extract*

To further identify the underlying mechanism of sFRP2 in regulating cell inflammation and Th17/Treg balance, we detected its effect on the cellular localization and expression of β-catenin and Cyclin D1 in the isolated PBMCs. The immunofluorescence staining showed that both nuclear and cytosolic β-catenin were presented in control PBMCs, while CSE exposure resulted in less β-catenin expression neither nuclear nor cytosolic forms. The further si-sFRP2 transfection increased the β-catenin expression and more nuclear β-catenin was observed. Besides, we found that Cyclin D1 was mainly distributed in cell nucleus, which was enriched in control cells and decreased after CSE stimulation, while increased in response to sFRP2 inhibition (Fig. 4A). Western blot analysis showed that expression of β-catenin and Cyclin D1 decreased in PBMCs exposed to CSE. Knockdown of sFRP2 markedly increased expression of β-catenin and Cyclin D1, compared with the si-NC group (Fig. 4B-4C). Moreover, inhibition of the Wnt/β-catenin pathway by inhibitor DKK-1 markedly decreased β-catenin and Cyclin D1 levels in PBMCs (Fig. 4D-4E). Inhibition of Wnt/β-catenin pathway decreased concentrations of IL-6 and TNF-α in PBMCs (Fig. 4F). Further study demonstrated that inhibition of Wnt/β-catenin reversed the effect of sFRP2 silencing on Th17, Treg, and Th17/Treg percentage, as indicated by the increased frequency of Th17 cells (Fig. 4G), decreased frequency of Treg cells (Fig. 4H), and increased ratio of Th17/Treg cells (Fig. 4I). Collectively, these results indicated that the Wnt/β-catenin pathway participated in the inhibitory effect of si-sFRP2 on cell inflammation and Th17/Treg imbalance.

## 4. Discussion

The present study showed that sFRP2 increased in the serum of patients with COPD and in HBE cells exposed to CSE and that sFRP2 was inversely correlated with FEV1/FVC. Reducing sFRP2 downregulated the Th17/Treg ratio via the Wnt/β-catenin pathway.

The sFRP family of secreted glycoproteins have seven members: sFRP1, sFRP2, sFRP3, sFRP4, sFRP5, sFRP6 and sFRP7. These glycoproteins inhibit Wnt signaling by competitively binding to the frizzled receptors of cell membranes. Recent research has shown that reduced expression of frizzled receptor 4 prevents Wnt- and β-catenin-driven alveolar lung repair in COPD (Skronska-Wasek et al., 2017). The sFRP glycoproteins also play roles in autoimmune and inflammatory diseases. For example, sFRP1(-/-) mice exhibit aberrant mesenchymal proliferation and impaired alveoli formation (Foronjy et al., 2010). Specifically, sFRP5 suppresses inflammation in rheumatoid arthritis fibroblast-like synoviocytes by downregulating the c-Jun N-terminal kinase (Kwon et al., 2014). Additionally, sFRP5 diminishes cardiac inflammation and protects the heart from ischemia and reperfusion injury (Nakamura et al., 2016). These results indicate a potential role of sFRPs in immune disease.

The structural and cellular changes observed in lungs of COPD patients phenotypically resemble the accelerated aging of the organ.

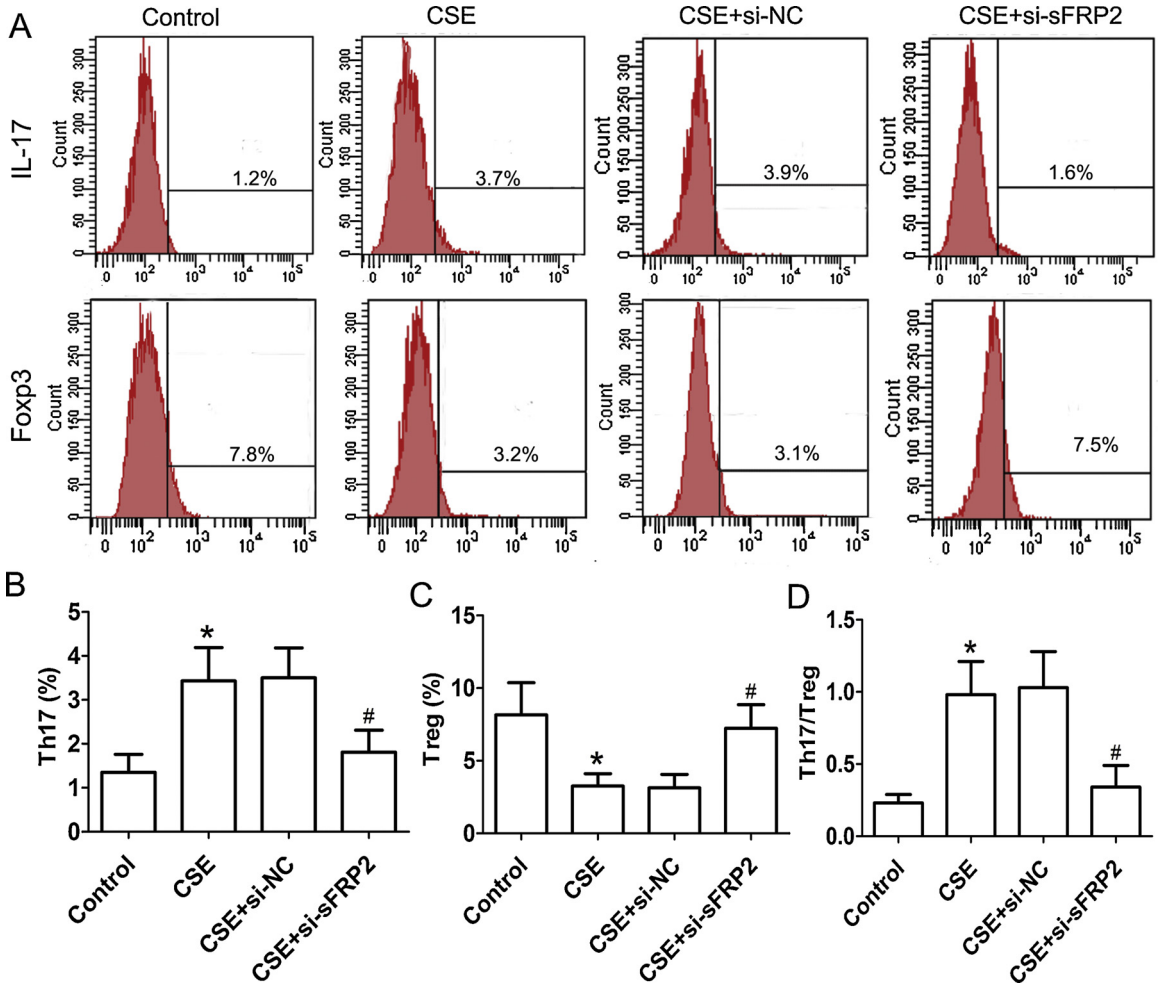


**Fig. 3.** Knockdown of sFRP2 suppressed the frequencies of Treg cells and Th17 cells. Peripheral blood mononuclear cells were isolated and transfected with 60 nM of sFRP2-siRNA (si-sFRP2) for 48 h. PBMCs then were exposed to cigarette smoke extract for 24 h and treated with a PMA/ionomycin mixture (4 μL/mL) for an additional 6 h. After sorting for $CD3^+CD8^-$ and $CD4^+CD25^+$ cells, $IL\text{-}17^+$ and $Foxp3^+$ cells were stained and detected using flow cytometry. (A) Representative images $IL\text{-}17^+$ and $Foxp3^+$ cells percentage in the corresponding T cell populations; Ratio of Th17/$CD3^+$CD8- cells (B) and Treg/$CD4^+CD25^+$ cells (C) was determined using flow cytometry. (D) Representative column chart of Th17/Treg ratio. $^{*}P < .05$ versus the control group; $^{\#}P < .05$ versus the CSE + si-NC group. Data represent results from four independent experiments.

Interestingly, age-related increases in sFRP2 promote oxidative stress and potentiate both angiogenesis and metastasis in melanoma cells (Kaur et al., 2016). Thus, we hypothesize a potential role of sFRP2 in the pathogenesis of COPD. The present data demonstrated significantly increased sFRP2 in the serum of patients with COPD patients and up-regulated sFRP2 in HBE cells exposed to CSE. We also found CSE induced the sFRP2 mRNA and protein in a dose and time dependent manner and sFRP2 mRNA and protein levels changed in a similar trend at indicated CSE dose and treatment time. I considered that the transcription and translation are two highly dynamic process, and the mRNA level closely correlate with the protein level when the post-transcriptional modifications are not defined. We also found higher baseline levels of sFRP2 mRNA, which may reflect that at the indicate time point more mRNA accumulated than the resulted protein, although their amount could not be compared in the same dimension. These results indicate that CSE is a positive regulator of sFRP2 expression, which is consistent with previous research confirming expression of sFRP2 in smokers with COPD (Wang et al., 2011).

Wnt/β-catenin signaling is believed to play critical roles in COPD. This signaling regulates CSE-induced airway inflammation via the PPARδ/p38 pathway (Guo et al., 2016). The present study demonstrated that sFRP2 induced inflammatory cytokines by inhibiting the Wnt/β-catenin pathway. However, whether sFRP2 is an antagonist or agonist to β-catenin remains a matter of debate. Findings from studies on angiosarcoma and triple-negative breast cancer suggest that sFRP2 monoclonal antibody inhibits the activation of β-catenin in tumors (Fontenot et al., 2013). However, sFRP2 augments β-catenin activities initiated by WNT16B instead of directly altering canonical Wnt signaling (Sun et al., 2016). This contradiction may be related to different cell lines and sFRP2 concentrations. In tissues with low levels of sFRP2 expression, sFRP2 appears to augment Wnt signaling while to inhibit Wnt at higher sFRP2 levels (Mastri et al., 2014).

sFRP2 regulates the balance of Th17/Treg via the Wnt/β-catenin signaling pathway. In mice, Wnt/β-catenin pathway promotes lipopolysaccharide-induced acute lung injury by driving the Th17 response (Cheng et al., 2018). Blockade this pathway aggravates silica-induced lung inflammation via Treg regulation of the Th immune response (Dai et al., 2016). In dendritic cells, Wnt signaling regulates Th1 and Th17 responses and suppresses autoimmune neuroinflammation (Suryawanshi et al., 2015). Thus, the Wnt/β-catenin pathway may help to regulate $CD4^+$ T cell subset differentiation. Moreover, sFRP1 promotes human Th17 differentiation (Lee et al., 2012). In the present study, we demonstrated that knockdown of sFRP2 downregulated the proportion of Th17/Treg cells.

Findings of the present study underscore the importance of SFRP2 as a mediator of airway remodeling in COPD. sFRP2 also contributes to

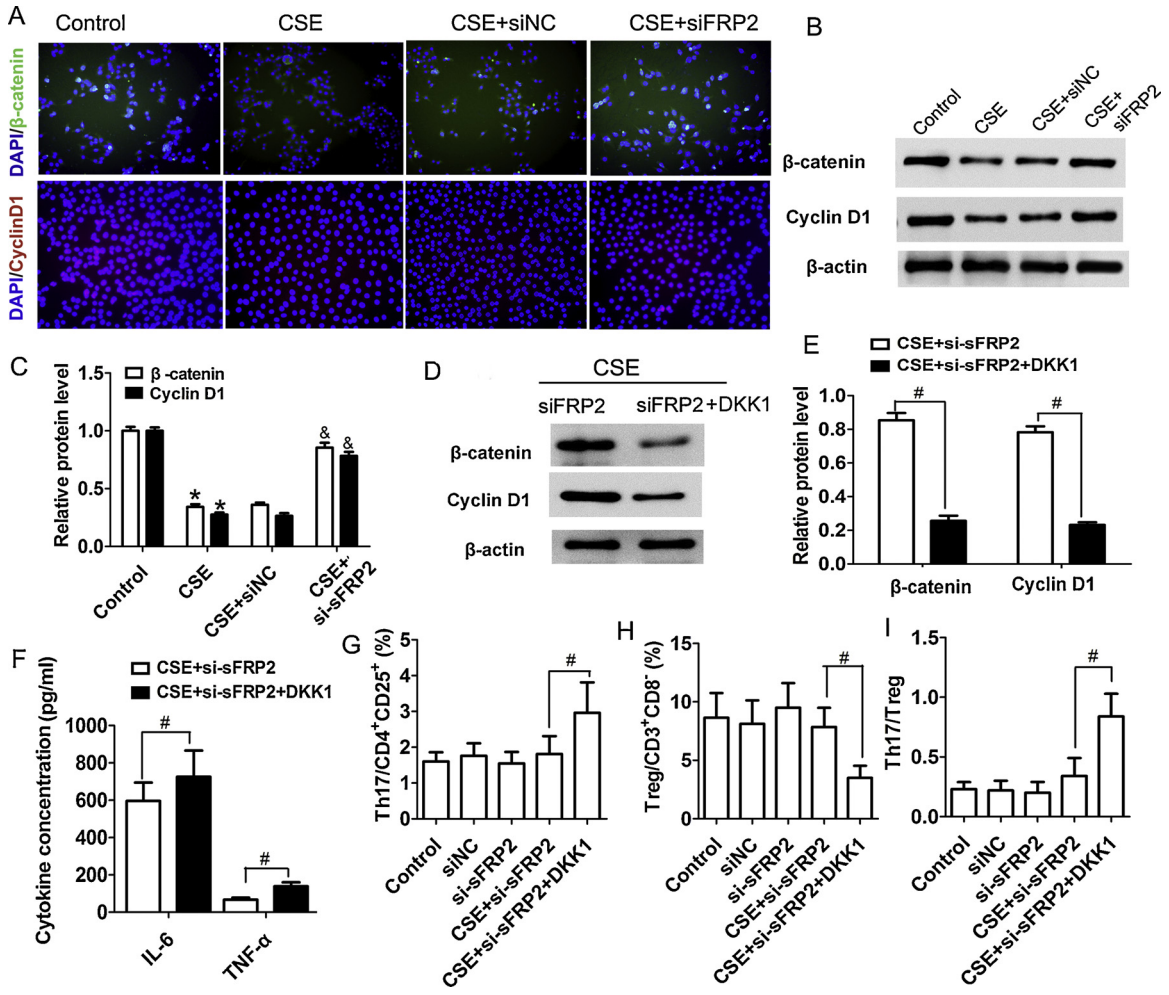


**Fig. 4.** sFRP2 regulated the inflammatory response and Th17/Treg ratio by inhibiting the Wnt/β-catenin pathway. PBMCs were transfected with 60 nM of sFRP2 siRNA (si-sFRP2) for 24 h and exposed to cigarette smoke extract for 24 h. The PBMCs were then treated with a PMA/ionomycin mixture (4 μL/mL) for an additional 6 h before examinations. (A) Cellular localization of β-catenin and Cyclin D1 in PBMCs, the cell nucleus were stained with DAPI. (B–C) Relative expression of β-catenin and Cyclin D1 in PBMCs cells was analyzed by western blot. Cells were transfected with si-SFRP2, followed by treatment with the Wnt/β-catenin antagonist, Dickkopf-1 (DKK1). The cells then were exposed to cigarette smoke extract. (D–E) Relative expression of β-catenin and Cyclin D1 was assessed by western blot. (F) The inflammatory cytokines IL-6 and TNF-α in the supernatant of the HBE cell culture were analyzed by corresponding ELISA kits. PBMCs cells were transfected with sFRP2-siRNA (si-sFRP2) for 48 h. Flow cytometry was used to determine ratio of Th17/$CD3^+CD8^-$ cells (G) and Treg/$CD4^+CD25^+$ cells (H). (I) Representative column chart of the Th17/Treg ratio. $^*P < .05$ versus the control group; $^{\&}P < .05$ versus the si-NC group; $^{\#}P < .05$ versus the CSE + siNC group; $^{\#}P < .05$. Data represent results from four independent experiments.

COPD by disturbing the balance between Th17 and Treg cells by modulating the Wnt/β-catenin pathway. As the decrease of gene expression of sFRPs is often associated with promoter hypermethylation (Surana et al., 2014). The relationship between the expression change of sFRP2 and its methylation needs further exploration. Additionally, HBE cells may produce and secrete various inflammatory mediators or cytokines, which potentially affect the T cell differentiation and immunological response, however, the association and crosstalk between HBE cells and T cells should be elucidated in more details in the further studies. Inhibition of sFRP2 via epigenetic modifying agents may provide a promising therapeutic strategy for COPD.

## Declaration of Competing Interest

All authors declare that they have no potential conflict of interests.

## Acknowledgement

This work was supported by the Special project of traditional Chinese medicine research in Henan province (No. 2018ZY1004; No. 2018ZY2104).

## References

Ballweg, K., et al., 2014. Cigarette smoke extract affects mitochondrial function in alveolar epithelial cells. Am. J. Physiol. Lung Cell Mol. Physiol. 307 (2014), L895–907.
Barnes, P.J., 2016. Inflammatory mechanisms in patients with chronic obstructive pulmonary disease. J. Allergy Clin. Immunol. 138 (2016), 16–27.
Capozzolo, A., et al., 2017. Clinical and functional lung parameters associated with frequent exacerbator phenotype in subjects with severe COPD. Respir. Care 62 (2017), 572–578.
Cheng, L., et al., 2018. Wnt/beta-catenin pathway promotes acute lung injury induced by LPS through driving the Th17 response in mice. Biochem. Biophys. Res. Commun. 495 (2018), 1890–1895.
Dai, W., et al., 2016. Blockade of Wnt/beta-Catenin pathway aggravated silica-induced lung inflammation through tregs regulation on Th immune responses. Mediators Inflamm. 2016 (2016), 6235614.
Fontenot, E., et al., 2013. A novel monoclonal antibody to secreted frizzled-related protein 2 inhibits tumor growth. Mol. Cancer Ther. 12 (2013), 685–695.
Foronjy, R., et al., 2010. The divergent roles of secreted frizzled related protein-1 (SFRP1) in lung morphogenesis and emphysema. Am. J. Pathol. 177 (2010), 598–607.
Guo, L., et al., 2016. WNT/beta-catenin signaling regulates cigarette smoke-induced airway inflammation via the PPARdelta/p38 pathway. Lab. Invest. 96 (2016), 218–229.
Kaur, A., et al., 2016. sFRP2 in the aged microenvironment drives melanoma metastasis

and therapy resistance. Nature 532 (2016), 250–254.
Kwon, Y.J., et al., 2014. Secreted frizzled-related protein 5 suppresses inflammatory response in rheumatoid arthritis fibroblast-like synoviocytes through down-regulation of c-Jun N-terminal kinase. Rheumatology (Oxford) 53 (2014), 1704–1711.
Lee, Y.S., et al., 2012. The Wnt inhibitor secreted Frizzled-Related Protein 1 (sFRP1) promotes human Th17 differentiation. Eur. J. Immunol. 42 (2012), 2564–2573.
Li, X.N., et al., 2014. Imbalances of Th17 and Treg cells and their respective cytokines in COPD patients by disease stage. Int. J. Clin. Exp. Med. 7 (2014), 5324–5329.
Mastri, M., et al., 2014. Secreted Frizzled-related protein 2 as a target in antifibrotic therapeutic intervention. Am. J. Physiol., Cell Physiol. 306 (2014), C531–539.
Miao, C., et al., 2018. DNA hypermethylation of SFRP2 influences the pathology of rheumatoid arthritis through the canonical Wnt signaling in model rats. Autoimmunity (2018), 1–14.
Nakamura, K., et al., 2016. Secreted frizzled-related protein 5 diminishes cardiac inflammation and protects the heart from Ischemia/Reperfusion injury. J. Biol. Chem. 291 (2016), 2566–2575.
Saetta, M., et al., 1993. Activated T-lymphocytes and macrophages in bronchial mucosa of subjects with chronic bronchitis. Am. Rev. Respir. Dis. 147 (1993), 301–306.
Skronska-Wasek, W., et al., 2017. Reduced frizzled receptor 4 expression prevents Wnt/beta-Catenin-driven alveolar lung repair in chronic obstructive pulmonary sisease. Am. J. Respir. Crit. Care Med. 196 (2017), 172–185.
Sun, Y., et al., 2016. SFRP2 augments WNT16B signaling to promote therapeutic resistance in the damaged tumor microenvironment. Oncogene 35 (2016), 4321–4334.
Surana, R., et al., 2014. Secreted frizzled related proteins: implications in cancers. Biochim. Biophys. Acta 1845 (2014), 53–65.
Suryawanshi, A., et al., 2015. Canonical wnt signaling in dendritic cells regulates Th1/Th17 responses and suppresses autoimmune neuroinflammation. J. Immunol. 194 (2015), 3295–3304.
Takagi, H., et al., 2008. Frequent epigenetic inactivation of SFRP genes in hepatocellular carcinoma. J. Gastroenterol. 43 (2008), 378–389.
Vargas-Rojas, M.I., et al., 2011. Increase of Th17 cells in peripheral blood of patients with chronic obstructive pulmonary disease. Respir. Med. 105 (2011), 1648–1654.
Vestbo, J., et al., 2013. Global strategy for the diagnosis, management, and prevention of chronic obstructive pulmonary disease: GOLD executive summary. Am. J. Respir. Crit. Care Med. 187 (2013), 347–365.
Vogelmeier, C.F., et al., 2017. Global Strategy for the Diagnosis, Management, and Prevention of Chronic Obstructive Lung Disease 2017 Report. GOLD Executive Summary. Am. J.Respir. Crit. Care Med. 195 (2017), 557–582.
Wang, C., et al., 2018. Prevalence and risk factors of chronic obstructive pulmonary disease in China (the China Pulmonary Health [CPH] study): a national cross-sectional study. Lancet 391 (2018), 1706–1717.
Wang, H., et al., 2015. Imbalance of peripheral blood Th17 and Treg responses in patients with chronic obstructive pulmonary disease. Clin. Respir. J. 9 (2015), 330–341.
Wang, R., et al., 2011. Down-regulation of the canonical Wnt beta-catenin pathway in the airway epithelium of healthy smokers and smokers with COPD. PLoS One 6 (2011), e14793.
Weaver, C.T., Hatton, R.D., 2009. Interplay between the TH17 and TReg cell lineages: a (co-)evolutionary perspective. Nat. Rev. Immunol. 9 (2009), 883–889.
Zeng, X., et al., 2018. Secreted frizzled related protein 2 modulates epithelial-mesenchymal transition and stemness via Wnt/beta-Catenin signaling in Choriocarcinoma. Cell. Physiol. Biochem. 50 (2018), 1815–1831.